ARCTIC
VOL. 79, NO. 1 (MARCH) P. 10–30
https://doi.org/10.14430/arctic83882

Monitoring Lake Ice and Snow in the Canadian High Arctic Using Digital Camera Imagery

Brianna E. Lane[1] and Laura C. Brown[1,2]

(*Received 4 October 2025; accepted in revised form 5 March 2026*)

ABSTRACT. In the Arctic region, a decline in ice and snow cover has been observed in recent years, resulting in adverse effects on the climate, hydrological events, biological processes, and human populations. Monitoring changes in ice and snow cover using satellite imagery or models is common, while novel research is beginning to use ground-based camera systems for in situ monitoring of cryosphere elements. This study focused on maximizing the use of ground-based time-lapse imagery from trail cameras for ice and snow studies from 2016 to 2022 within the context of the changing Arctic climate. We monitored lake ice and snow at five lakes (Resolute Lake, Small Lake, North Lake, Plateau Lake, and Hunting Camp Lake) near Resolute and Nanuit Itillinga, Nunavut, in the Central Canadian High Arctic. We developed a semi-automated technique that uses image classification tools to quantify the progression of ice and snow extent in the camera view. Image classification yielded an overall classification accuracy of 86%, and a Kappa coefficient of 0.79 from nearly 13,000 images, indicating a strong and viable monitoring system despite some variance in performance from viewing conditions. Lake ice and snow phenology dates determined from classified imagery had averages generally within a few days of observations (mean bias error of 2–9 days). Average ice duration was 308 days (20 September–25 July), and average snow duration was 298 days (14 September–8 July). The camera-based data extraction technique is a viable tool, not only for tracking long-term changes in snow and ice conditions, but also for validating satellite or modelling work in other logistically challenging environments. Thus, this methodology to monitor Arctic ice and snow phenology can support better projections for future responses to climate change.

Keywords: lake ice; snow; digital imagery; trail cameras; image classification

RÉSUMÉ. Des études menées dans la région arctique ont révélé une baisse de la couverture de neige et de glace au cours des dernières années, ce qui entraîne des conséquences néfastes sur le climat, les événements hydrologiques, les processus biologiques et les populations humaines. La surveillance des variations de la glace et de la neige grâce à des images satellitaires ou à des modèles est une pratique courante. Des études récentes ont commencé à utiliser des systèmes de caméras installées sur le sol pour surveiller directement des éléments de la cryosphère. Cette étude s'est concentrée sur l'optimisation de l'utilisation de l'imagerie accélérée capturée par des caméras installées sur des sentiers pour les études de la glace et de la neige effectuées de 2016 à 2022 dans le contexte du climat changeant de l'Arctique. Nous avons surveillé la glace lacustre et la neige de cinq lacs (lac Resolute, lac Small, lac North, lac Plateau et lac Hunting Camp) situés près de Resolute et de Nanuit Itillinga, au Nunavut, dans la région centrale de l'Extrême-Arctique canadien. Pour quantifier la progression de la superficie de glace et de neige capturée par les caméras, nous avons mis au point une technique semi-automatisée de classification d'images. La classification des images a permis d'obtenir un taux d'exactitude global de 86 % et un coefficient Kappa de 0,79 à partir d'environ 13 000 images, ce qui suggère un système de surveillance solide et viable malgré certaines variations de rendement sur le plan des conditions d'observation. Les moyennes des dates de la phénologie de la glace lacustre et de la neige, obtenues à l'aide des images classifiées, se situaient généralement à l'intérieur d'un écart de quelques jours par rapport aux observations (erreur de justesse moyenne de 2 à 9 jours). La durée moyenne de la glace était de 308 jours (du 20 septembre au 25 juillet), tandis que la durée moyenne de la neige était de 298 jours (du 14 septembre au 8 juillet). La technique d'extraction de données à l'aide de caméras est un outil viable non seulement pour suivre à long terme l'évolution des conditions de la neige et de la glace, mais aussi pour valider les résultats obtenus au moyen de satellites ou de modélisations dans des environnements logistiquement difficiles. Par conséquent, cette méthode de suivi de la phénologie de la glace et de la neige de l'Arctique peut contribuer à des projections améliorées concernant les réponses futures au changement climatique.

Mots-clés : glace lacustre; neige; imagerie numérique; caméras de sentiers; classification des images

Traduit pour la revue *Arctic* par Nicole Giguère.

[1] Department of Geography, Geomatics and Environment, University of Toronto Mississauga, 3359 Mississauga Road, Mississauga, Ontario L5L 1CG, Canada
[2] Corresponding author: lc.brown@utoronto.ca

INTRODUCTION

The rapid warming of the Arctic is an increasing concern. Currently, the Arctic region is warming at a rate four times the global average since 1979 (Rantanen et al., 2022), resulting in a decline in both the extent and duration of ice and snow in recent years (Wang et al., 2022; Young, 2023). This loss has negative implications for large-scaled phenomena such as the global climate, due to feedbacks from decreased surface reflectivity (albedo) (Brown and Duguay, 2010; Young, 2023); hydrological events, such as timing of melt and freeze (Geldsetzer et al., 2010); lake ecology, including species' habitat conditions and interactions (Hampton et al., 2017); and hazards faced by human communities related to transportation routes and recreational activities (Brown and Duguay, 2010).

Lake ice duration is projected to decrease considerably by the end of the century (Huang et al., 2022). Other phenological changes include later freeze-up and earlier break-up in the Northern Hemisphere (e.g., Benson et al., 2012; Dauginis and Brown, 2021). One study recorded greater changes in far northern lakes compared to other Canadian lakes, specifically later freeze-up (Latifovic and Pouliot, 2007), highlighting the need for increased focus on northern sites. Snow cover is expected to follow similar trends, with projections estimating that, by the end of the century, rain will become the dominant form of precipitation in the Arctic (McCrystall et al., 2021). Additionally, recent studies indicate that the timing of snow cover is already shifting in the Canadian Arctic (e.g., Dauginis and Brown, 2021), and decreases in spring snow cover extents have been reported across the pan-Arctic and Northern Hemisphere (Mudryk et al., 2020, 2022). Therefore, due to the interconnected nature of the Arctic system, monitoring snow and ice is crucial.

Over the past 40 years, there has been a decline in ground-based lake ice monitoring in Canada (Lenormand et al., 2002) and other pan-Arctic countries (Prowse et al., 2011; Murfitt and Duguay, 2021), with spatial coverage and representation particularly limited in the Canadian Arctic. Similarly, snow cover observations, including measurements of snow water equivalent and precipitation, are restricted by spatial and temporal gaps (Bokhorst et al., 2016).

Logistical challenges (such as inaccessibility and remoteness) and harsh environmental conditions in the Arctic promote the use of satellite imagery and modelling (e.g., Arp et al., 2010; Du et al., 2017; MacKay et al., 2017; Zhang et al., 2021), which can be valuable for extensive monitoring. However, despite the many applications of off-site methods, the need for observation-based ground data to validate satellite imagery and modelling data remains.

Previous research has documented the extent and coverage of lake ice and snow using satellite imagery and model-based approaches (e.g., Brown and Duguay, 2010). But spatial and temporal resolution limits restrict data (Xiao et al., 2018), and modelling may not be able to simulate local lake-specific conditions without prior knowledge of the snow conditions (e.g., Robinson et al., 2021). Meanwhile, innovative research is starting to make use of digital camera imagery for in situ monitoring, such as using automated cameras to study changing lake and river ice (Ansari et al., 2017; Xiao et al., 2018; Ariano and Brown, 2019). Ground-based cameras are relatively affordable, straightforward to install, and generally offer higher resolution than space-based platforms (Xiao et al., 2018), enabling detection of subtle regional variations (e.g., ice and snow redistribution on smaller lakes). However, previous studies using ground-based cameras for monitoring have faced challenges during the freeze–melt transition, when lakes are only partially frozen (Xiao et al., 2018), and in applying methods across different lakes (Tom et al., 2020).

Landcover classification is a widely used tool in remote sensing. Earlier research in northern Canada has explored various classification techniques to evaluate land cover in relation to ecological structure and to classify ecosystems (Atkinson and Treitz, 2012; Chasmer et al., 2014; Bothmann et al., 2017; Hung and Treitz, 2020). While landcover classification remains popular for ecological studies in the Canadian Arctic, fewer investigations have focused on lake ice through image classification for cryosphere monitoring. Examples include supervised classification of lake ice cover at the Great Lakes in Canada (Leshkevich and Nghiem, 2013), the application of a random forest machine learning algorithm at Qinghai Lake in China (Han et al., 2020) and employing random forest classifiers to track lake ice globally from MODIS (Wu et al., 2021). Remote sensing already offers a valuable method for monitoring lake ice and snow (e.g., Mudryk et al., 2020; Murfitt and Duguay, 2021), and there is great potential to extend this approach with ground-based cameras, and to broaden it to other cryosphere observations. The objectives of this research were to develop a feasible method for extracting ice and snow phenology from a large volume of in situ digital imagery, and to validate this new approach against manually extracted snow and ice phenology from the imagery. In so doing, we also sought to assess the accuracy and practicality of the in-situ method for studying recent phenological changes in the Central Canadian High Arctic.

METHODOLOGY

Study Area

Field research was carried out on five lakes in the Central Canadian High Arctic: Resolute Lake, Small Lake, North Lake, and Plateau Lake near the community of Resolute or Qausuittuq, Nunavut (74˚ 41′ 45″N, 94˚ 49′ 45″W) on the southern coast of Cornwallis Island, along with Hunting Camp Lake in Nanuit Itillinga (formerly Polar Bear Pass) National Wildlife Area (75˚ 44'N, 98˚ 25'W) on Bathurst Island (Fig. 1). This study area is a low-elevation polar desert ecoregion with limited vegetation growth

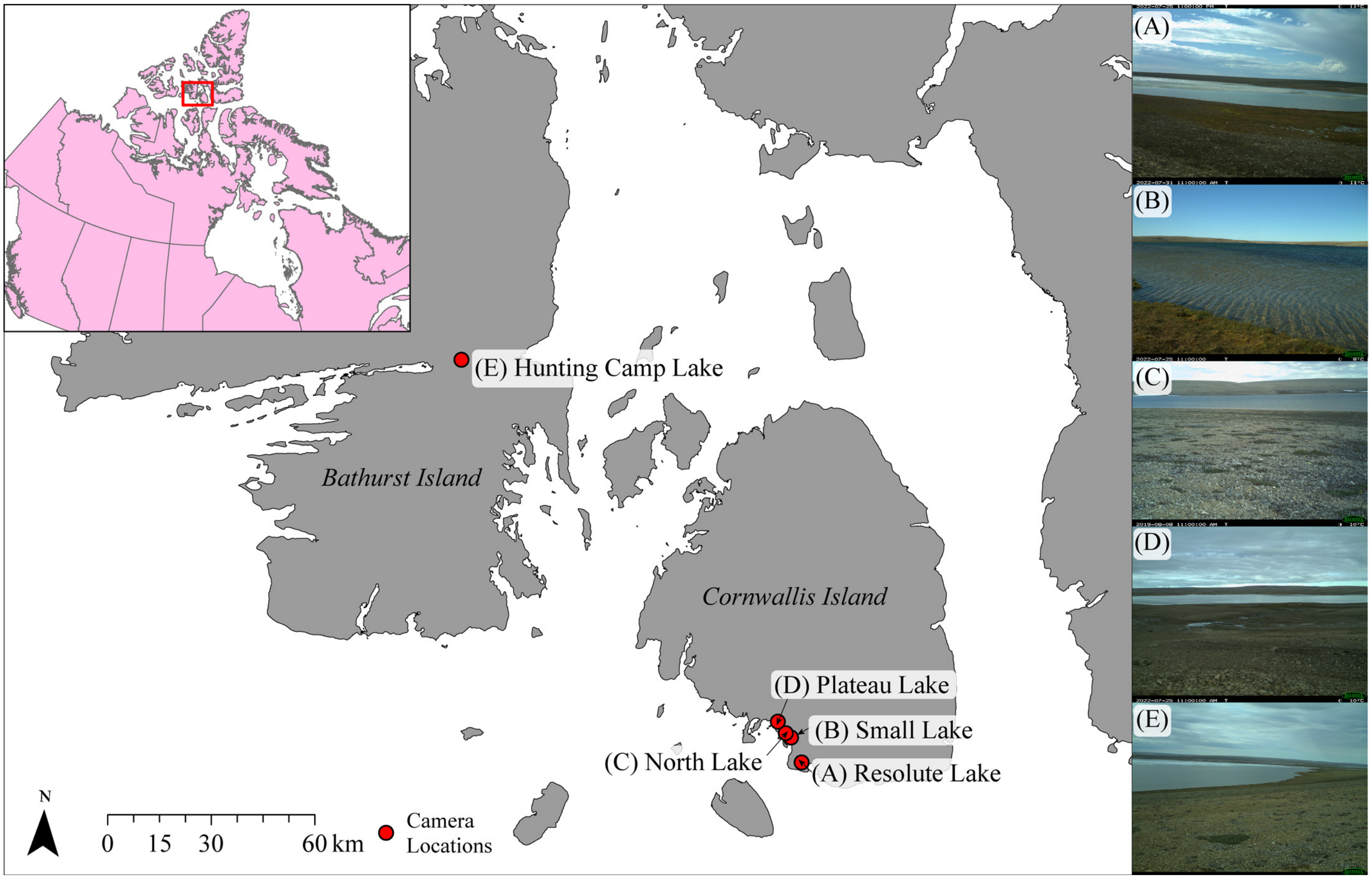

FIG. 1. Location of field sites on Bathurst Island and Cornwallis Island. Red markers represent the location of the cameras. An example of digital imagery from each camera is given on the right for (A) Resolute Lake, (B) Small Lake, (C) North Lake, (D) Plateau Lake, and (E) Hunting Camp Lake. Base map source: Statistics Canada. Available online: https://www12.statcan.gc.ca/census-recensement/2011/geo/bound-limit/bound-limit-2016-eng.cfm

(French and Slaymaker, 2011; Young et al., 2018). Based on data from 1991 to 2020, the daily average temperatures in Resolute are 4.9˚C in July and –32.1˚C in February, the warmest and coldest months, respectively (ECCC, 2022). Precipitation mainly falls as snow (about 100 cm annually), with around 60 mm of rain each year; little precipitation occurs between November and April (ECCC, 2022). Nanuit Itillinga, where Hunting Camp Lake is located, has been identified as having overall similar weather and climate conditions to Resolute, despite being a polar semi-desert (Young and Labine, 2010). The terrain surrounding the wetlands varies in elevation from 23 m to 180 m above sea level (Young and Labine, 2010; Young, 2019).

Methods

We previously installed a series of Reconxy HyperFire outdoor cameras (PC800 HyperFire Professional IR and HyperFire 2 Professional HP2X), with one camera overlooking each of the five lakes (Table 1). The captured imagery spans a period of two to seven years (2016–22) and mostly consists of images taken twice daily at 11:00 a.m. and 1:00 p.m. Central Standard Time (CST) (Table 2). These times were selected to optimize visibility as day length shortens before the onset of polar night, the period of 24-hour darkness in winter. Exceptions include Resolute Lake, where images are taken once daily at 1 pm CST from 6 June 2018, onwards, and Plateau Lake and North Lake, where extra images were collected during the first phenological year of data collection (2019–20), with images taken on the hour from 6 am CST to 6 pm CST, though these additional images were only used as supplementary information. All cameras were installed in locations that afforded the best possible visibility of the lakes, based on accessibility (Ariano and Brown, 2019), following consultation with local representatives from the Resolute community. They were secured to rebar with cold-weather (–40°C) zip ties to ensure they remained stable through inclement weather and winter conditions (Fig. 2). The cameras, which remain in place as of this writing, with adjustments, and which continue to collect data for future analyses, are approximately 70 cm above the ground, a height chosen to minimize snow coverage on the lens while reducing wind interference common with taller poles. Duct seal putty was applied around each camera for added weatherproofing, and a protective casing was placed around the battery wire to limit power disruptions caused by wildlife chewing wires. Power was supplied by an external 12 V battery housed in a weatherproof box, covered with rocks for extra protection, with internal AA lithium

TABLE 1. The location of each camera and the corresponding lake characteristics. All sites are in Nunavut, Canada.

Lake name	Location	Latitude	Longitude	Elevation (m a.s.l.)	Camera orientation	Surface area (km²)	Maximum depth (m)	Mean depth (m)
Resolute Lake	Cornwallis Island	74.72˚N	94.95˚W	1.49	SE	1.27	22.5	7.9
Small Lake[1]	Cornwallis Island	74.76˚N	95.06˚W	18.52	W–SW	0.2*	9.7	4.1
North Lake[2]	Cornwallis Island	74.77˚N	95.11˚W	29.86	NE	0.6	18.5	5.4
Plateau Lake[3]	Cornwallis Island	74.80˚N	95.19˚W	44.06	NW	0.7*	18*	
Hunting Camp Lake	Bathurst Island	75.75˚N	98.56˚W	26.20	W–SW	4.5	2**	

* Lescord et al., 2015.

** Canadian Wildlife Service (2001). However, recent field measurements have recorded slightly greater than 2 m depths in parts of the lake.

Alternate names for lakes used locally: [1] Three Mile Lake; [2] Five Mile Lake; [3] Nine Mile Lake.

TABLE 2. The number and dates range of images available for each lake and the number of images removed (unusable) and used in classification (usable). Unusable images exclude images taken during polar darkness (November–February).

Lake	Starting date	Ending date	Total number of images	Unusable number of images	Usable number of images	Usable lake images (%)
Resolute Lake	31/07/2017	31/07/2022	2110	126	743	85.5
Small Lake	22/05/2016	30/07/2022	3910	632	2465	79.6
North Lake	06/08/2019	02/08/2022	6953	513	3566	87.4
Plateau Lake	05/08/2019	03/08/2022	10,239	491	3551	87.9
Hunting Camp Lake	25/05/2016	03/08/2022	4518	508	2641	83.9
Total			27,730	2270	12,966	85.1

FIG. 2. Example setup of the Reconxy HyperFire outdoor camera (Photos: A. Robinson).

batteries serving as backup in case the external power failed (one camera is powered solely by AA batteries).

Ground-truthing surveys were conducted during the summers of 2021 and 2022. Ground truthing was conducted at Resolute Lake on 12 August 2021, with 10 ground control points (GCPs). An additional camera was positioned in front of the installed camera to replicate the view (without disrupting the original camera positioning or programming) and capture imagery of the GCPs. Ten rebar pieces, each with bright orange fabric attached for enhanced visibility in the imagery (Fig. 3), were placed at known distances from the camera, and their GPS coordinates were recorded using a Garmin eTrex 10 GPS (Accuracy ±10 m, 95% confidence interval). These data supplied coordinates at known points used for scale as reference points during image analysis. This process was repeated at Small Lake on 7 August 2022, and North Lake on 10 August 2022. Logistical constraints prevented the collection of similar GCPs at Plateau Lake and Hunting Camp Lake.

Figure 4 shows the processing flow for each image. During preprocessing, image quality was assessed manually to determine usability based on visibility and view. Images were considered poor quality if the camera lens was covered by rain or snow, or if weather was too foggy or hazy to see the lake within the frame. Our criterion for selecting photos for classification was that a photo had at least a partial view of the far side of the lake. Images where the view shifted due to the camera turning in strong wind were still used in most cases. Photos taken during the polar night were excluded.

Georectification, the process of adding geographic information to the image, was completed using multipoint geometric correction, a feature available in ERDAS Imagine 2022 (ERDAS). One image from each lake (Resolute Lake, Small Lake, and North Lake) was manually georeferenced by adding the GCPs obtained during field sampling. These reference images were used to acquire spatial information (i.e., surface area of each class; data not included in this manuscript) from the remaining images, as current limitations of the software prevent automation of georectification between raw images. The final product was resampled during geometric transformation using Nearest Neighbour sampling (Parker et al., 1983). Note that georectification is not required for phenology extraction.

A combination of supervised training and unsupervised classification (K-means) produced the best results and

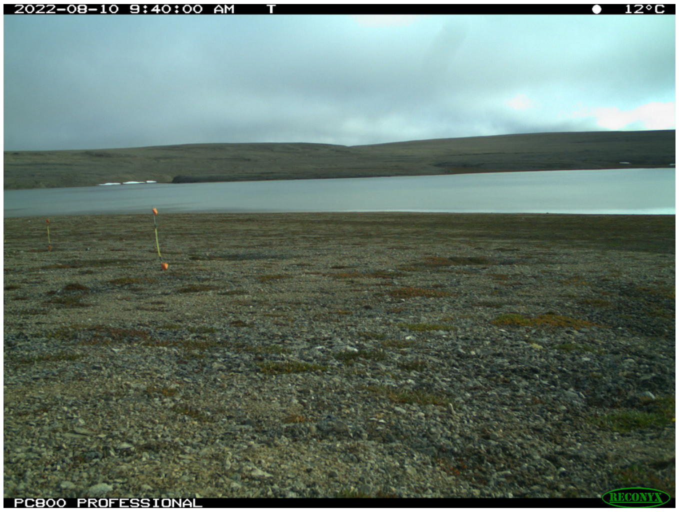

FIG. 3. Example of the rebar with flags positioned for the ground truthing survey at North Lake. Image taken by a PC800 HyperFire Professional IR camera.

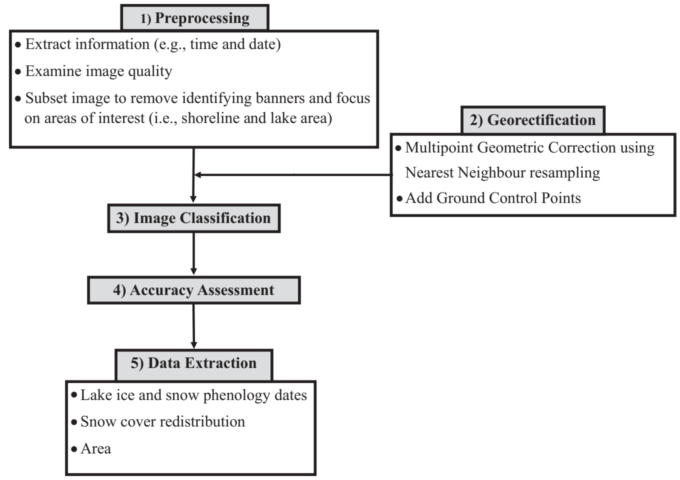

FIG. 4. Analysis process for camera imagery repeated for all five lakes except for georectification, which was completed only at Resolute Lake, Small Lake, and North Lake.

TABLE 3. Error matrix created from the final signature files based on supervised training data.

Reference Data (%)	Classified Data (%)			
	Snow	Shore	Water	Ice
Snow	96.26	0.04	3.56	2.76
Shore	0.02	98.80	3.06	0.00
Water	0.97	1.14	85.21	2.15
Ice	2.76	0.02	8.17	95.09
Total	100.00	100.00	100.00	100.00

usability through the automated classification processes within ERDAS. A total of 40 training samples, representing spectral data from the four desired classes (snow, ice, water, shore) covering a mix of weather conditions and transitional ice states, were collected as user-defined polygons from 10 random images of Resolute Lake and Small Lake. Some images contained multiple classes. We assumed these training samples were transferable across lakes due to their similar environmental context (i.e., close in latitude, ecological zone) and similar overall ground cover, snow and ice conditions. Signature files, which define the training samples, were created with 10 examples for each class from 10 different images; these images included varying conditions over the study years, such as sunny, cloudy, and foggy weather, as well as during the transition time for freeze–melt. After creation, the signatures were evaluated using contingency or error matrices, and manual adjustments—such as combining, splitting, or merging training samples—were made to optimize classification performance. The final signature used in the classification was formed by merging several prior mid-processing signatures into one (Fig. 4, Step 3) after achieving a sufficient accuracy level based on the error matrices (Hexagon, 2024). The contingency matrix subsequently provides a means to assess how well the training samples align with the anticipated classification (Table 3) (Brereton, 2021). This error matrix indicated that the classes matched between 85.21% and 98.80%. On average, water was misclassified as ice in 8.17% of samples, while the other classes experienced misclassification rates of less than 5%.

Once the training data were selected, a spatial model was developed to automate the unsupervised classification process within ERDAS using the K-means method, with classes (clusters) defined by the signature files created through the supervised training process (settings are included in Table S1). In previous cases, supervised classification outperformed unsupervised classification in land cover classification (Mohd Hasmadi et al., 2009); however, through our methodology development, a hybrid classification method yielded the best results.

Within the classification model, areas of interest were cropped to include only the lake and shoreline, which varied between the lakes and across different years. The resulting classified images contained categories interpreted as one of the following: shore, water, ice, snow, or unclassified, which referred to pixels not belonging to the other four classes (e.g., sky, banners on images). Some images were excluded due to an Eigenvector classification error in the processing components of ERDAS (specifically, the inability to invert the covariance matrix, indicating that the single-layer image was too homogeneous [n = 96]) as well as during post-classification due to poor image quality (n = 60). Overall, 85.1% of the usable camera images taken were incorporated into the classification process, leaving only 14.9% of the dataset unusable for the analysis (see Table 2).

Following image classification, we performed accuracy assessments in the software to validate the results. To calculate classification accuracy, including overall accuracy and a Kappa coefficient, we generated 250 stratified random reference points (Congalton, 1991) (independent from training data) from 30 randomly selected images (six images per lake). This indicated the improvement of the classification over random chance. Our choice to use 30 images to assess classification quality followed Ansari et al. (2017), who also examined freshwater ice using shore-based

TABLE 4. Lake ice and snow phenology definitions used in this paper.

Term	Definition
Freeze-up	The transition period between the first appearance of ice on the lake until the lake was completely frozen over.
Snow-on period	The intermittent snow fall period between first snow-on and final snow-on.
First on	The first appearance of ice or snow.
Final on	The date of complete ice or snow cover.
Lake ice/snow cover duration	The number of days between the final ice/snow-on to final ice/snow-off.
Break-up	The transition period between the first appearance of open water until the lake was completely ice-free.
Snow-off period	The time between first snow-off to final snow-off.
First off	The first sign of open water or bare ground.
Final off	The date when the lake was entirely ice-free or the terrain was snow-free for the remainder of the season.

cameras. In the random selection process, these images were screened to ensure representation of all classes and environmental conditions. We define poor classification as an accuracy below 70%, adequate classification as 70%–79%, and good classification at 80% or above.

We used daily class information from each image to extract phenology dates, which we compared with manually identified lake ice and snow phenology dates to assess the accuracy of the automated class detection. Other studies have also validated phenology dates using experienced manual/visual interpretation, a reliable observation method (e.g., Ansari et al., 2017; Han et al., 2020). Root mean square error (RMSE) and mean bias error (MBE) were used to quantify the error between the manually extracted (observed) dates and the dates generated by the classification method.

Two dates were identified to describe each freeze-up and break-up period (Table 4), namely, the first appearance, or disappearance of ice or snow, and the final appearance, or disappearance, following other cryosphere studies (e.g., Dauginis and Brown, 2021), with appearance and disappearance defined in this study as anywhere in the analysis field of the camera image. The first and final dates do not always differ; for example, the first snow-on and final snow-on dates could be the same for snow phenology if a melt did not occur after the first snow-on.

Areas of ice relative to water, and snow cover relative to shore areas were calculated within ERDAS to quantify lake ice and snow coverage, with coverage presented here as percentages for comparison over time.

RESULTS

Image Classification

Accuracy Assessments: Across all lakes and years of sampling, average classification accuracy was 86%, with a Kappa coefficient (κ) of 0.79. The highest accuracy recorded was 98.8%, with a κ of 0.98 for an image taken at Small Lake in October 2016 (Table S2). This image contained only snow. Classification results perform well when there is only one or two classes in a single image. Figure 5a was captured when Resolute Lake was covered in ice and snow, showing the program's ability to distinguish between ice and snow with high accuracy, even under low-light conditions. Figure 5b depicts an image where high classification accuracy and κ are reported, taken during the open water season at Small Lake.

The lowest classification accuracy was 29.6%, with a κ of 0.12 (Fig. S1). This image was taken at Small Lake in July 2022 during ice break-up. Conditions were cloudy, with ice and snow visible in the image. Both the highest- and lowest-performing classifications used images from Small Lake. In the particularly poorly classified image, clouds reflected on the lake, which was mainly open water, resulting in a spectral reflectance similar to snow (see Nicodemus, et al., 1977; Kimes, 1983). Previous studies have also identified errors for classes that spectrally resembled each other (Hung and Treitz, 2020). We included all images taken throughout the summer (after ice break-up) to maintain consistency in the landscape and to improve training classes during snow-on and snow-off periods by including examples with the snow-free shore.

Errors during transition periods have been observed by others (Xiao et al., 2018) and were responsible for two poor accuracy assessments in our study lakes (Resolute Lake on 14 June 2018, and Small Lake on 19 June 2018). However, the transition period examples at Hunting Camp Lake showed favourable classifications (classification accuracy $\geq$ 73.6%, κ $\geq$ 0.65). Figure 5e provides an example demonstrating the effectiveness of high-quality training samples in distinguishing between ice and snow during break-up. Better visibility and separation between classes at Hunting Camp Lake are likely due to the camera position, as it is situated on an elevated ridge overlooking the lake. However, this position also led to errors caused by reflections. Although transition periods sometimes had lower accuracy, this was not a consistent pattern across all lakes or transition period images. Table 5 presents the accuracy assessments for each lake, on average, and indicates that Resolute Lake had the highest classification accuracy, while Small Lake had the lowest. Interestingly, the κ does not follow the same pattern. North Lake and Hunting Camp Lake had equal κ values (see Table 5), and Small Lake had the lowest κ. Camera elevation relative to the shoreline factored into the poor classification results at Small Lake, particularly during transition periods, as the camera is positioned at lake level near the shore, whereas the other lakes have a higher vantage point (Table 1).

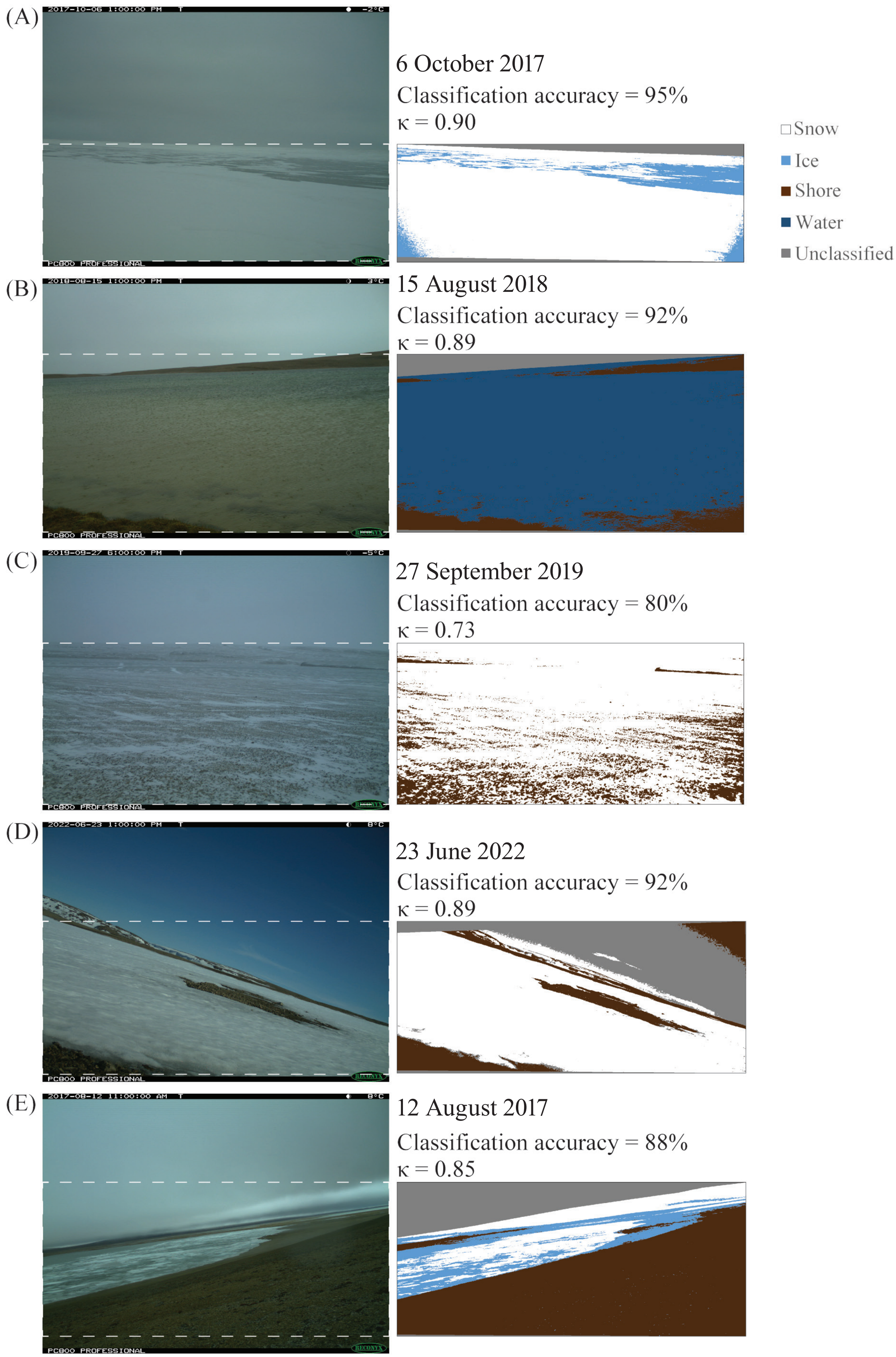

FIG. 5. Examples of digital camera imagery (left) and resulting classified image (right). Classified extent noted with dashed white line. Results from (A) Resolute Lake, (B) Small Lake, (C) North Lake, (D) Plateau Lake, and (E) Hunting Camp Lake.

TABLE 5. Average accuracy assessment results for each of the five lakes.

Lake	Classification accuracy (%)	Kappa coefficient (κ)
Resolute	89.13	0.81
Small	76.16	0.63
North	88.00	0.84
Plateau	87.00	0.83
Hunting Camp	87.73	0.84
Average	85.61	0.79

One common factor in misclassification was the presence of cloud cover, which could be misclassified as snow (e.g., Fig. 5e, where the strip of brighter clouds is misclassified as snow) or reflected on the lake's surface and misclassified as snow. Another source of misclassification occurred with sunny conditions, where sun glare could occur on the lake and was occasionally quantified as snow. Yet, in some cases, cloudy conditions performed better than sunny conditions (as seen on Small Lake on 16 October 2016, for example). Further training samples could be beneficial to reduce this issue, as could adjusting the image brightness, depending on the ground conditions; however, this additional labour contradicts the goal of automating the process.

In some cases, local community members and other researchers serviced the cameras by realigning them back to their intended view angle or removing accumulated snow that blocked the lens, which would not have been possible for inaccessible cameras. The ability to classify well, even when the camera view shifted, was valuable. For example, at Plateau Lake, classification results could still track the movement of snow across the landscape, as demonstrated in Figure 5d. The view appeared off centre with no lake in the frame (16 June – 3 August 2022), but still provided good visibility of the snow on the shore and the snowmelt period. Additionally, images with low visibility still produced adequate-to-good classification results. For example, two photos taken during October (transition period) at Resolute Lake had classification accuracies above 93% and κ above 0.90, higher than the average classification accuracy and κ for Resolute Lake (Table S2). In general, image colour changed when the sun was at its lowest point on the horizon at North Lake and Plateau Lake. The low sun angle did not affect image classification quality, as evident in Figure 5c. Thus, similar to Wu et al. (2021), we have demonstrated that ground-based cameras are a suitable alternative to mitigate issues, typically encountered with satellite imagery, of the low zenith angle.

Class Distribution and Surface Cover: Quantifying ice and snow in the imagery can provide a valuable understanding of spatial and temporal change in the study area. Seasonal phenology is evident in the imagery at all lakes: periods of snow retreat are visible before snow-free lake ice appears, followed by melt; then, open water and snow-free shorelines become visible (Fig. 6). Additionally, changes in surface cover are evident in snow-covered versus bare ice (Fig. 7), and in snow coverage of the lake and its surrounding shoreline (Fig. 8) throughout the year. These figures demonstrate detailed information on the ice and snow cover on the lakes with a high temporal resolution. For example, during the freeze-up period in 2017 at Resolute Lake, bare ice was recorded, as shown in Figure 7. In contrast, the ice was entirely snow-covered during formation in 2018. Thus, the snow cover disappearing on ice is evident and detectable based on the classification method, which enables detection and tracking of snow cover retreat and advance on ice, thereby enhancing understanding of the phenology of these lakes more than is possible from space-based imagery.

Manual Extraction vs. Image Classification Results: On average, the first ice-on dates identified by the classification method had an MBE of just three days later than the manually extracted dates (Table 6), while the final ice-on dates had an MBE of three days earlier than the manually extracted dates, indicating that full ice cover was reported slightly before lakes were entirely frozen. For the first ice-off, the classification method had an MBE of only two days earlier (noting that the year-to-year fit was quite variable), while for the final ice-off, the classification method had an MBE of five days earlier than observed. Combining the ice-on and ice-off timings for all five lakes results in an overall average ice cover duration only three days' different between the classified and manually extracted dates (308 vs. 311 days).

The first snow-on showed the greatest discrepancy between the two identification methods, with the classification method detecting snow eight days later (MBE) than the manually observed dates and also having the second-highest RMSE among all snow and ice phenology parameters (Table 7). However, the final snow-on date was detected well, only two days later (MBE) than the manually extracted dates. The snow-off detection performed well overall but exhibited some variability; overall, the classification method detected the first snow-off two days later (MBE), and the final snow-off two days earlier (MBE). Overall, snow cover duration was noted as being just two days shorter using the classification method (298 vs. 300 days).

Some differences stem from camera positioning and errors related to sun glare. Despite these issues, classification results in this work show that using ground-based cameras is a feasible and valuable method for automating ice phenology extraction from a large dataset, while grounded in experienced manual interpretation.

Phenology Comparisons

Lake Ice: Freeze-up: Ice-on dates were not synchronized across the lakes, with greater variability between lakes for first ice than for final ice cover (Fig. 9a and 9b). The primary factor influencing freeze-up under similar climate conditions is lake morphometry (Brown and Duguay, 2010); shallower lakes tend to freeze earlier under the same climate forcing (Huang et al., 2022). Hunting Camp Lake, being shallow (around 2 m deep), can lose heat to the atmosphere

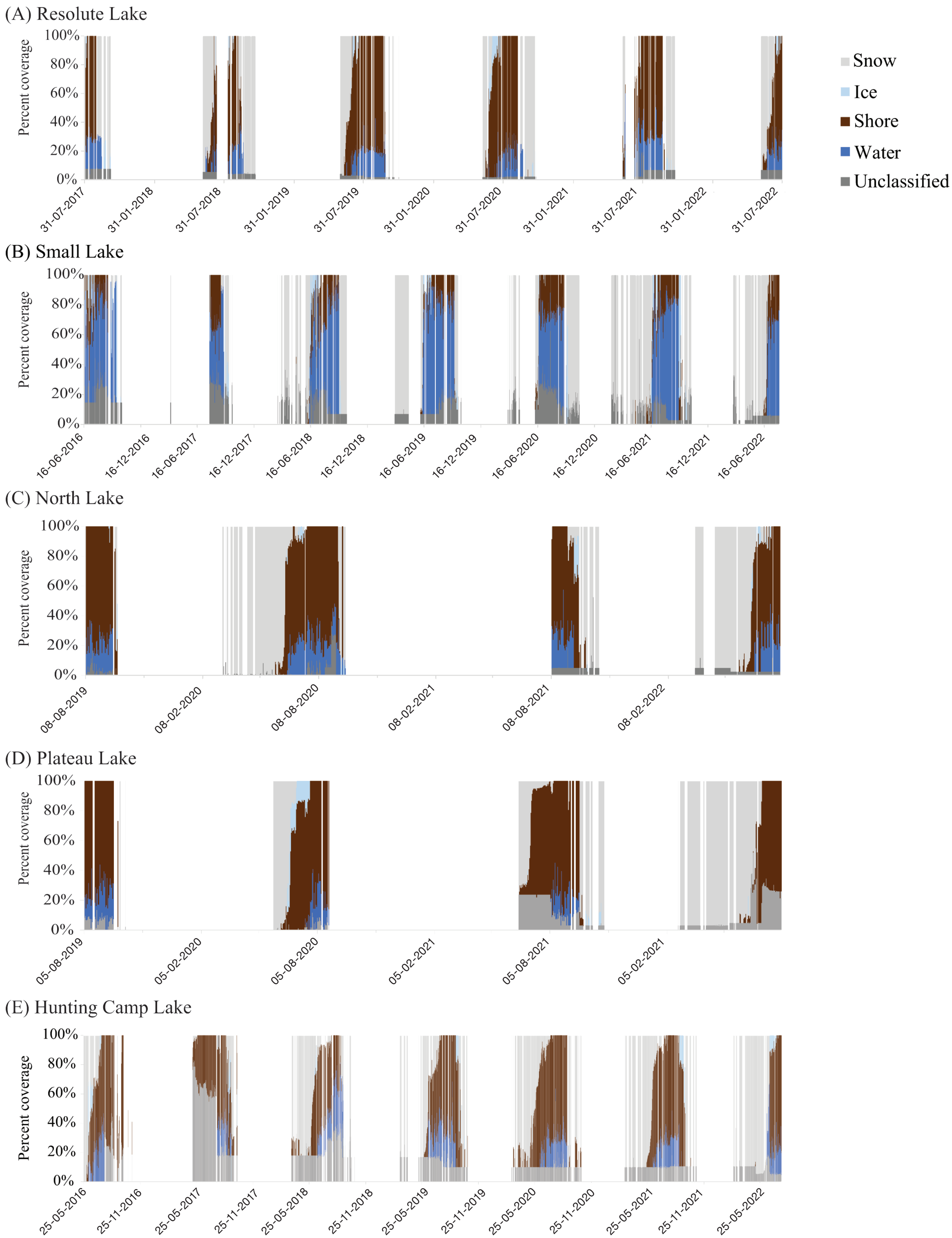

FIG. 6. Percentage coverage of each category for the entire data period from all lakes. White space represents polar darkness, power interruptions, or camera malfunctions. Note different timescales, as not all cameras were set up in the same year.

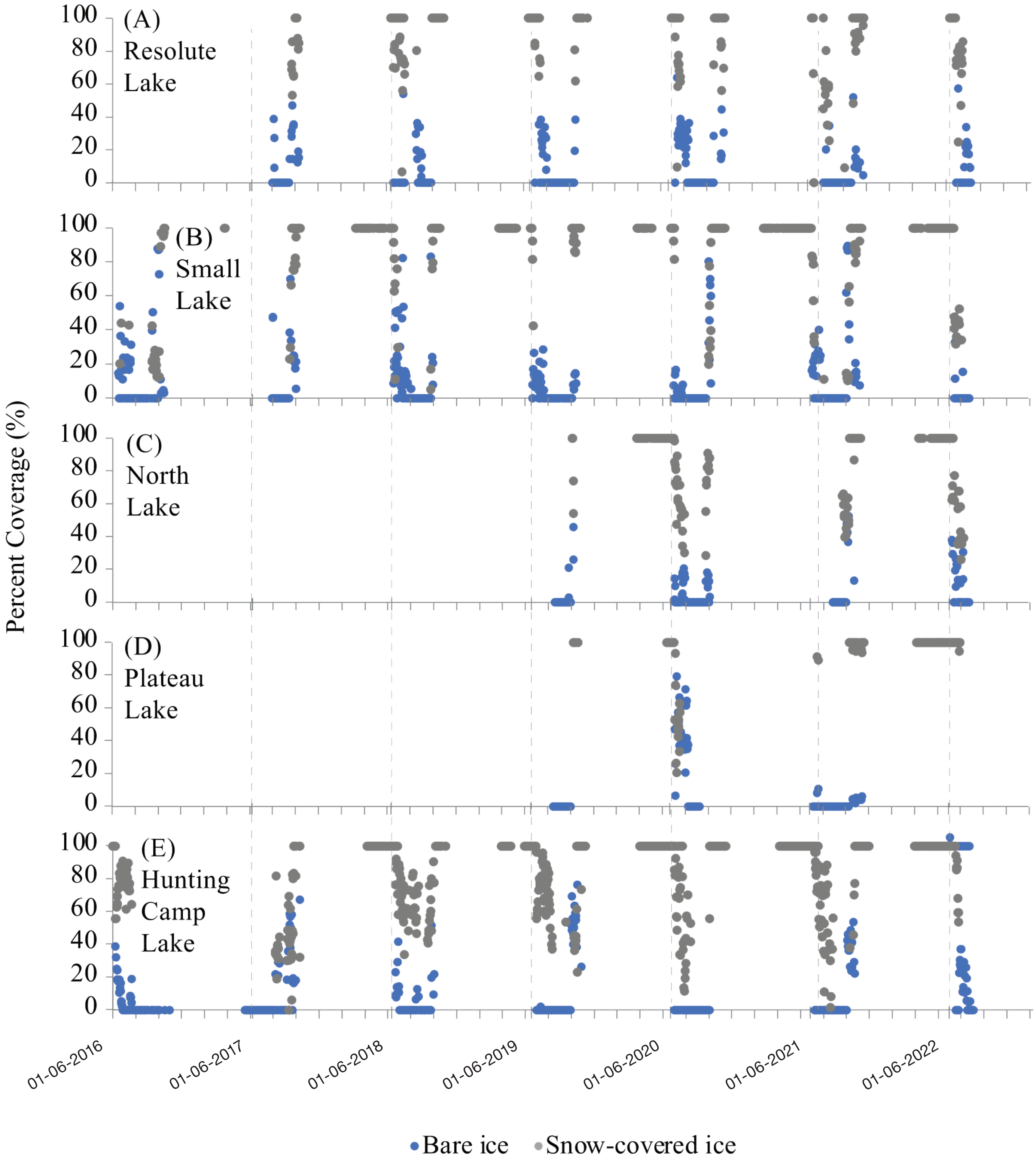

FIG. 7. Lake ice surface cover for the five lakes for all years, with available data based on classification results. Blue circles represent bare ice coverage, and grey circles represent snow-covered ice. For each year, 1 June is indicated by the vertical dashed line.

more quickly, causing water to cool and freeze faster than in deeper lakes. As shown in Table 6, the mean first ice-on date for all five lakes was 17 September, compared to the manually observed average of 11 September. The final average ice-on dates ranged from 14 September at Hunting Camp Lake to 30 September at Plateau Lake. This range is slightly broader than the observed range at the same lakes, but the overall inter-lake average differed by only two days between the two methods (Table 6).

The freeze-up period averaged four days across all lakes

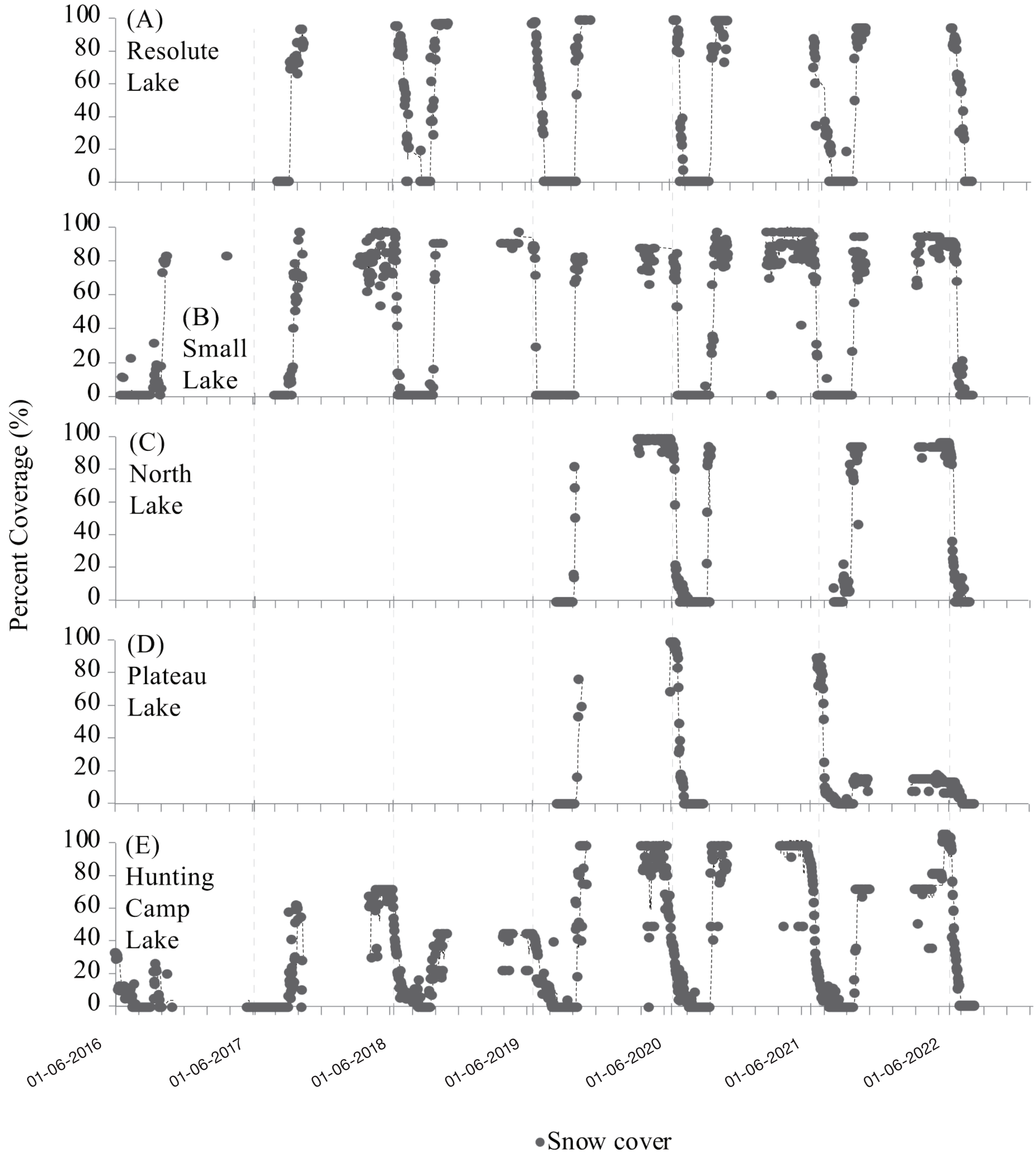

FIG. 8. Snow surface cover for the five lakes for all years, with available data based on classification results. Grey circles represent snow coverage. To enhance visual clarity of the seasons, black dotted line represents five-day moving averages. For each year, 1 June is indicated by a vertical dashed line.

and years, based on the classification dates. In contrast, the manual method yielded a longer freeze, with 11 days for ice freeze-up, due to the earlier detection of ice using the observation method. Hunting Camp Lake had the longest freeze-up rate (close to 30 days in some years) and was influenced by the freeze seasons during 2017, 2018 and 2019, where an incomplete ice cover was present, with one small section of open water persisting into September (Fig. 10). Furthermore, the camera was covered by snow for several days in 2017 and 2018, and a complete freeze may

TABLE 6. Average lake ice phenology dates for all lakes and study years. + only 1 year of data for Plateau. Each year is listed in Tables S3 and S4.

Lake	First ice-on				Final ice-on				First ice-off				Final ice-off			
	Manual	Classified	RMSE	MBE	Manual	Classified	RMSE	MBE	Manual	Classified	RMSE	MBE	Manual	Classified	RMSE	MBE
Resolute	16 September	23 September	6.4		25 September	24 September	2.8		29 June	03 July	8.5		06 August	31 July	6.5	
Small	12 September	15 September	3.5		20 September	20 September	4.7		18 June	15 June	4.1		24 July	17 July	7.2	
North	09 September	12 September	1.4		22 September	17 September	7.3		19 June	18 June	1.4		21 July	17 July	3.6	
Plateau	16 September	28 September	6.1		26 September	30 September	5.0		18 June	20 June	2.0 +		27 July	25 July	2.0 +	
Hunting Camp	04 September	10 September	0.6		20 September	14 September	9.8		27 June	18 July	11.9		02 August	30 July	3.3	
All lakes	11 September	17 September	4.3	2.7	22 September	20 September	6.2	–2.7	23 June	22 June	7.7	–1.7	30 July	25 July	5.6	–4.6

Lake	Average ice cover duration (days)		Average freeze-up season (days)		Average break-up season (days)	
	Manual	Classified	Manual	Classified	Manual	Classified
Resolute	313	310	8	0	36	27
Small	308	301	7	5	37	32
North	303	302	13	5	32	31
Plateau	300	10	0	39	35	
Hunting Camp	317	320	17	6	35	19
All lakes	311	308	11	4	36	32

TABLE 7. Average snow phenology dates as day-of-year for all lakes and study years. Each year is listed in Tables S5 and S6.

Lake	First ice-on				Final ice-on				First ice-off				Final ice-off			
	Manual	Classified	RMSE	MBE	Manual	Classified	RMSE	MBE	Manual	Classified	RMSE	MBE	Manual	Classified	RMSE	MBE
Resolute	04 September	10 September	6.5		14 September	14 September	0.4		09 June	12 June	2.9		15 July	16 July	5.7	
Small	30 August	10 September	16.5		10 September	14 September	5.4		25 May	28 May	10.3		10 July	26 June	15.6	
North	03 September	16 September	16.9		11 September	16 September	0.6		21 May	14 May	4.5		09 July	29 July	3.0	
Plateau	03 September	15 September	19.8		18 September	15 September	1.0		15 May	29 May	14.0		09 July	11 July	2.0	
Hunting Camp	25 August	29 August 29	7.3		10 September	12 September	1.4		18 May	28 May	7.4		07 July	13 July	18.1	
All lakes	31 August	07 September	12.2	7.7	12 September	14 September	3.6	1.6	25 May	28 May	7.7	1.8	10 July	08 July	13.0	–1.9

Lake	Average ice cover duration (days)		Average freeze-up season (days)		Average break-up season (days)	
	Manual	Classified	Manual	Classified	Manual	Classified
Resolute	302	305	10	4	37	29
Small	302	281	11	4	46	29
North	300	279	8	0	49	46
Plateau	286	300	15	0	55	43
Hunting Camp	300	317	15	14	49	53
All lakes	300	298	12	6	46	43

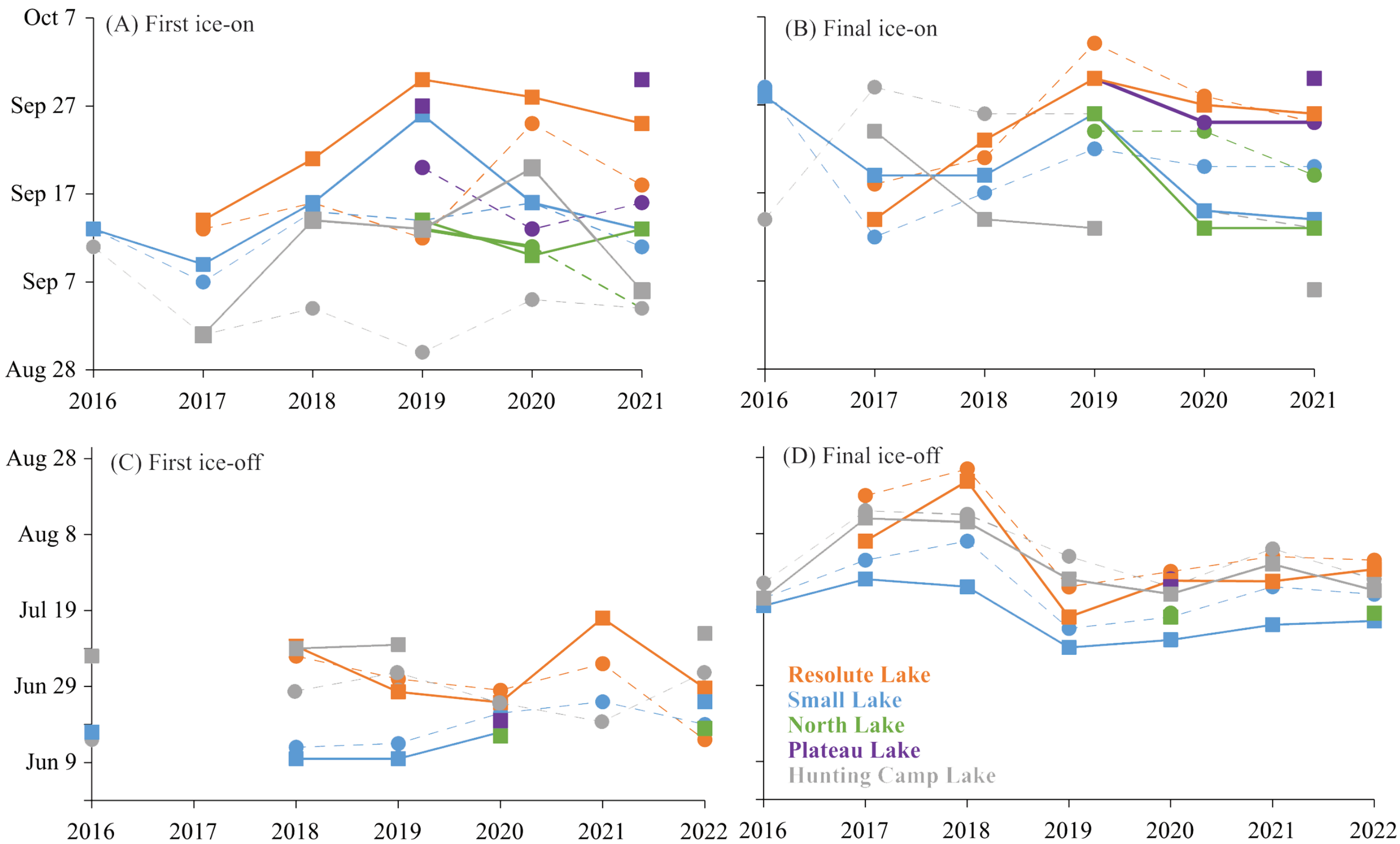

FIG 9. Classified phenology dates (squares) and manually extracted phenology dates (circles) for all five study lakes for a) first ice-on dates, b) final ice-on, c) first ice-off, and d) final ice-off.

have occurred while the view was obstructed, resulting in a later recorded date than the actual date.

Lake Ice: Break-up: In contrast to ice-on, ice-off was more synchronized between the lakes (Fig. 9c and d), as ice melt is primarily influenced by climate (Brown and Duguay, 2010). Across all lakes and years of data, the average first ice-off date was 22 June (23 June by observation method). The average final ice-off date was 25 July, five days earlier than the observation method (Table 6). Small and North Lakes had the earliest average final ice-off dates on 17 July (compared to 24 July for Small and 21 July for North using the observation method) (Table 6), while Resolute Lake had the latest on 31 July (versus 6 August by observation method).

The average final ice-off date for Small Lake is similar to the single date of 22 July 1981, reported in a previous study, when the lake was ice-free (Heron and Woo, 1994). At Hunting Camp Lake, the average first ice-off was identified as 18 June, but was observed manually from the imagery to be over a week later, on 27 June (RMSE 12 days). At this lake in particular, sun glare on the water or floating ice pan makes identifying the first ice-off difficult by observation, although classification accuracy was 87.7%, indicating good overall accuracy. This likely caused the discrepancy, as other lakes had first ice-off dates within four days of each other between methods. The average date for the appearance of open water on Hunting Camp Lake, as detected via satellite imagery from 1997 to 2011, was 25 June (Surdu et al., 2016). The mean final ice-off date from 1997 to 2011 was 26 July, close to recent years when the ice was fully gone by 30 July (classification method) or 2 August (observation method). The later dates result from the cameras' improved spatial resolution, which enables the detection of smaller remaining ice regions than those detected by satellites used in the comparable study, which had a finest resolution of 30 m (Surdu et al., 2016). These

FIG. 10. An open patch of water is still visible at Hunting Camp Lake, contributing to a longer freeze-up period and later final ice-on.

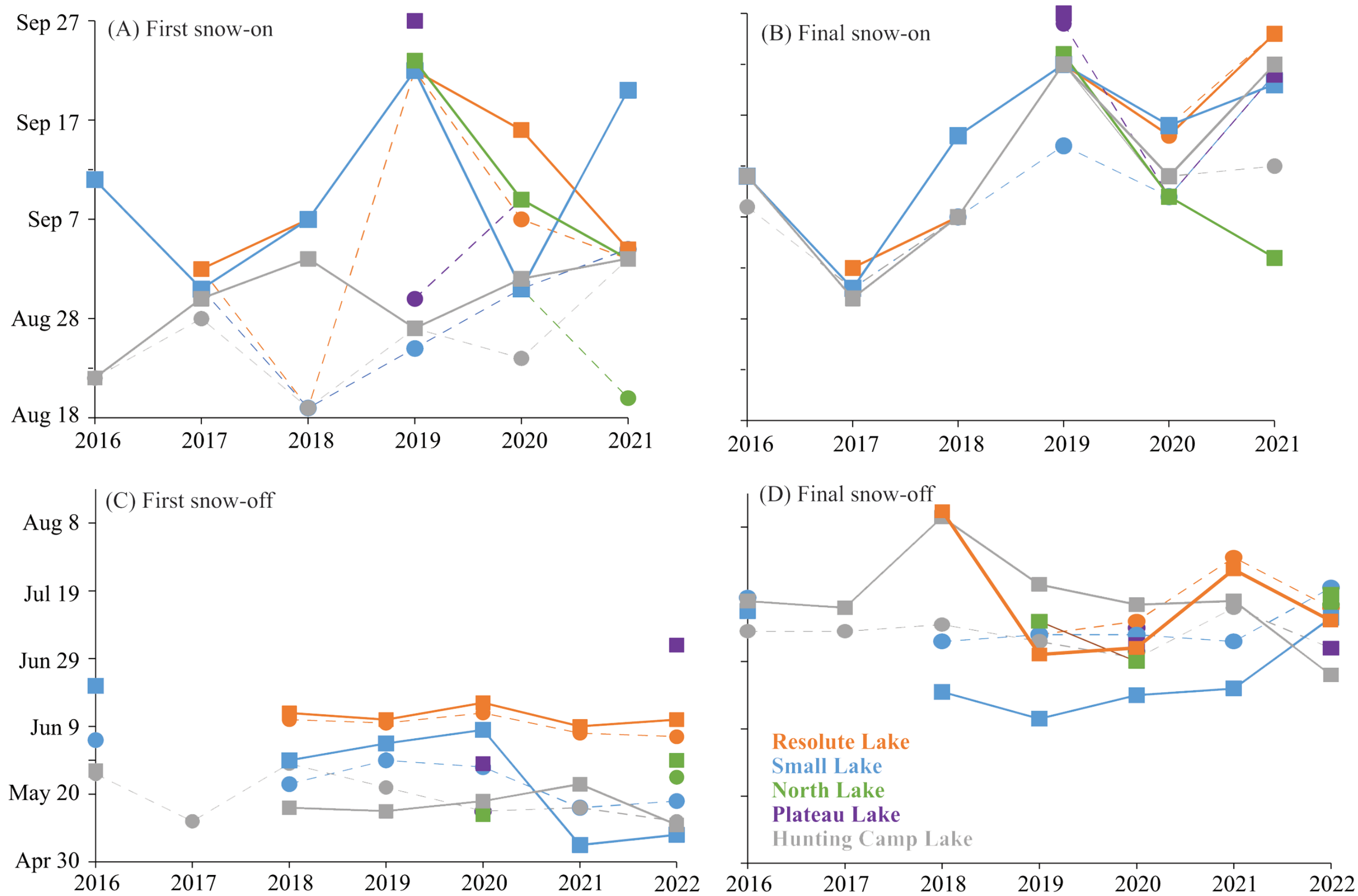

FIG. 11. Classified phenology dates (squares) and manually extracted phenology dates (circles) for all five study lakes for a) first snow-on dates, b) final snow-on c) first snow-off, and d) final snow-off.

ice-off dates are also similar to those of other lakes, such as West Lake and East Lake on Melville Island, where ice-off usually occurs in mid-July to early August (Dugan et al. 2012).

Compared to freeze-up, there was more variability in the break-up duration, with standard deviations of 11 and nine days, than in the freeze rates, with standard deviations of six and eight days (classified and observed, respectively) (Tables S3, S4). This difference is likely caused by the floating ice pans, which vary from year to year depending on melt rates and wind patterns during the break-up period.

Ice cover break-up duration lasted an average of 32 days (22 June–25 July) using the classification method, but four days longer with the observed method; of note, though, three additional years' first ice off dates were possible with the observed method, so some variation is expected. The classification method had difficulties with the 2018 ice-off season at Hunting Camp Lake, identifying the first ice-off date as 12 June, whereas observation indicated 28 June. The wet-looking, snow-free ice appeared bright blue this day from reflections and was misclassified as water, leading to a skewed break-up duration of 60 days, when it was 46 days from observation. This year was also particularly challenging to visually identify the beginning of break-up due to reflections on the ice near shore that made it difficult to distinguish water-on-ice from open water. Hunting Camp Lake had a slightly longer break-up duration than previously reported (29 days from melt onset to water clear of ice, Surdu et al., 2016), which is not unexpected, as our cameras can resolve more detail than the satellites used in that study.

Snow: Snow-on: For the landscape surrounding all five lakes, the average first snow-on date was 7 September, according to the classification method, and 31 August, based on the observation method. This parameter exhibited the second-highest RMSE and the largest MBE among all the phenology parameters (Table 7) (Fig. 11a, b). Final snow-on, however, was accurately detected using the classification method, with an average difference of only two days from observations, and the snow-on duration averaged six days (or 12 days when using the observation method) (Table 7).

Hunting Camp Lake experienced the earliest average snow-on date, on 29 August (25 August by observation method), which occurs about six weeks after the snow melted from the previous season. Overall temperature and precipitation conditions at Nanuit Itillinga are similar to those at Resolute (Young and Brown, 2023), but some differences in snowfall timing and duration are expected, as Hunting Camp Lake is approximately 140 km from the

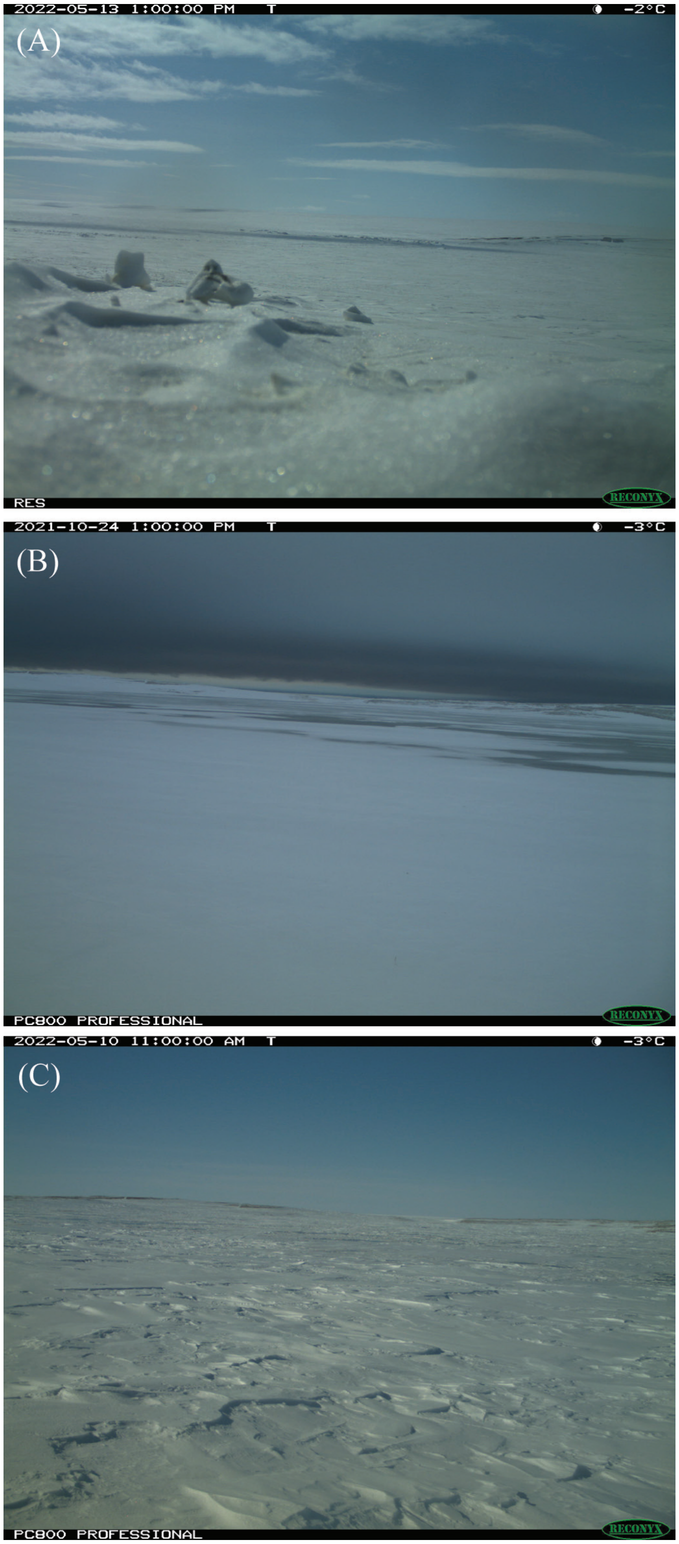

FIG. 12. (a) Resolute Lake from digital camera imagery on 13 May 2022. Snow depth is just below the lens of the camera; (b) view from Small Lake on 24 October 2021, and (c) 10 May 2022 (right). Snow redistribution is visible in the digital camera imagery over a phenological year.

other lakes.

While the small variability in average dates among the Cornwallis Island lakes, which are in relatively close proximity, can be explained by local precipitation variability, along with camera direction and local topography, the differences between the classification and observation methods highlight some challenges with detecting snow-on. These lakes showed an average snow-on of 10 days later using the classification method (12 September versus 2 September). The first and final snow-on timing is often the same using the classification method, whereas visually, in some years, a very small snowfall may be visible but is not recognized by the classification method. For example, at Plateau Lake in fall 2019, a light snowfall occurred on 30 August, leaving a small amount of snow in a topographic depression that quickly melted by the next day. The camera view was obscured (by snow and ice on the lens) from 21–26 September, but manual inspection revealed snow on the ground on 26 September visible through the haze. However, the image is not clear until 27 September, (the date detected using the classification method). Overall, as highlighted in Figure 11a and b, there is better coherence between the methods and the study lakes for detecting the final snow-on than the first snow-on.

Snow: Snow-off: Overall, both methods extracted comparable average days for first and final snow-off (differing by three days for the first snow-off and two days for the final snow-off). Yet, while the MBE was small, the RMSE was highest among all variables for snow-off, primarily due to errors related to Small Lake and Hunting Camp Lake caused by camera positioning.

The average first snow-off date was 28 May (25 May by observation method). Resolute Lake experienced the latest first snow-off with both methods (Fig. 11), while the earliest date varied between methods (North Lake by classification method, and Plateau by observation method). At Hunting Camp Lake, the average first snow-off date was 28 May (18 May by observation method), which is nearly a month earlier than a previous satellite-based study conducted at Polar Bear Pass (now Nanuit Itillinga) (using QuikSCAT, ~ 2.25 km resolution), which recorded 11 June as the start of snow-off from 2000–09 (Howell et al. 2012). Our finding demonstrates the enhanced ability for local-scale detection using ground-based imagery.

The average final snow-off date was 8 July, which is two days earlier than the date determined through observations. The earliest final snow-off with the classification method was Small Lake (26 June), while the earliest with visual inspection was Hunting Camp Lake (7 July). Once again, at Hunting Camp Lake, the improved resolution led to differences from the space-based final snow-off timing (Howell et al. 2012), with a difference of approximately one week using the ground-based data. Using ground-based manual observation dates for Hunting Camp Lake, snow offset lasted an average of 49 days from 2016 to 2022. In contrast, using space-based methods (for an earlier set of years) detected a 17-day offset period. This is an example of how ground-based imagery improves the ability to detect local land cover changes, such as bare patches of ground in late May, and persistent patches of snow toward the end of the melt season.

The final snow-off dates extracted through the classification method at Small Lake were heavily influenced by camera position and movement. The camera was placed very close to the shore, resulting in only a small shoreline segment where snow could be detected. During some years of melting, water levels rose above this shoreline segment. Additionally, the camera's position shifted slightly over the season, impacting the masked regions. The hills behind the lake contain small, late-lying snowbeds in topographic depressions, which are masked out in the classification method, leading to discrepancies between automated and visual detection. Using manual dates that only represent the small shoreline strip in the imagery aligns with the classification method for snow-off detection.

The large difference between classified and manually extracted dates at Hunting Camp Lake is due to sun glare. The floating ice pan in 2018 and 2020 reflected very brightly the day before the final snow-off, suggesting pixel values more indicative of snow. For comparison, removing incorrect classifications from the calculations restores the RMSE at Small and Hunting Camp Lakes to align with the other lakes, around five to six days.

For all the lakes, the average snow retreat period was similar, with only a three-day difference when using the classification method compared to the observation method.

Snow: Snow Cover Redistribution: Camera imagery revealed the variability in snow conditions on the study lakes. For example, snow decreasing around the Resolute Lake camera was visible through May 2022, despite many days when views were obstructed by snow at the height of the camera; when clear views were possible, the reduction in snow on the landscape was apparent (Fig. 12a). At Small Lake, imagery showed how conditions changed over the season, with patchy areas of ice visible in some parts and, at other times, snow that appeared compact and windblown, with sparse snow cover on the lake (Fig. 12 b, c). Combining the imagery with Figure 7 can provide a detailed explanation of snow cover redistribution throughout the season, which has implications for lake ice thickness below (e.g., Brown and Dugay, 2010).

Overall Duration and Relationships Between Ice and Snow: Despite the variation in ice detection between methods, average ice cover duration for all lakes combined was 308 days using the classification methods, and only three days later, at 311 days, using observations (Table 6). This finding is consistent with studies noting that ice duration can last over 10 months (Heron and Woo, 1994). Overall average snow cover duration (SCD) was just two days shorter using the classification method (298 days) than the observed method (300 days).

Some current studies have shown a decrease in SCD, with later snow onset and earlier snow offset in spring across the pan-Arctic (e.g., Liston and Hiemstra, 2011; Brown et al., 2021). Future predictions indicate a decrease in snow cover in Canada, especially during the spring months of April, May, and June (Mudryk et al. 2018). However, studies focusing on recent years (1997–2019) for the Canadian High Arctic (rather than the pan-Arctic) have shown that SCD changes were not statistically significant within the short time frame examined, although the timing shifted earlier, with earlier snow onset and melt (Dauginis and Brown, 2020, 2021). A lengthening of SCD occurred from 2006–13 in Nanuit Itillinga (Young et al., 2018), with earlier snow-on timing (though not statistically significant) and no change in snow-off noted when the record was extended through 2021 (Young and Brown, 2023). This discrepancy from other trends may be due to the short study period, as the long-term 40-year record from Resolute indicates both earlier snow-off and later snow-on (Young and Brown, 2023). Therefore, the subtle differences between study sites and time periods highlight the need for continuous Arctic monitoring, especially at the local scale, to track and understand emerging trends.

While the ice melt and snow retreat periods differed in duration by approximately 1.5 weeks, the snow retreat period began three weeks earlier (at the end of May), whereas ice began to visibly retreat in late June. Similarly, lake ice duration and SCD were also approximately 1.5 weeks different, at 308 days and 298 days, respectively. On average, snow cover was present for the season for about 1.5 weeks before ice formed a full cover, and it was fully gone from the landscape about three weeks before the ice cover was completely clear from the lakes (Tables 6 and 7). Considering these two cryosphere elements in tandem is essential, as snow acts as an insulator, inhibiting ice growth, while also delaying ice decay through its higher albedo when present on ice (Brown and Duguay, 2010; Serreze and Barry, 2014; Robinson et al., 2021).

DISCUSSION AND CONCLUSION

In this study, we present a novel and accessible semi-automated method for using remote sensing tools in conjunction with ground-based cameras. Our methodology for monitoring and quantifying snow and lake ice, a crucial activity in a changing Arctic environment, was straightforward and user-friendly. For nearly 13,000 images across five locations and several years, overall classification accuracy was 85.9%, with a Kappa coefficient of 0.79. Our methods can be applied to other disciplines related to tracking land cover changes, including glaciology and hydrology. Being able to quantify and track land cover changes throughout the year is particularly useful for ecological and biological studies. For example, shorebird breeding is closely tied to the 50% point of snow cover in the spring (Smith et al., 2010; Anderson et al., 2023), and the breeding season will be affected by changing snow cover conditions.

Lake ice and snow phenology dates determined from the classified camera imagery and validated based on experienced manual observations of the imagery aligned well, within two to five days for the ice phenology, and two to nine days for snow phenology. In general, aside from the noted classification errors discussed previously, first ice-on tended to be slightly earlier from visual inspection than using the classified method. One reason for this difference is, when using the classified method, there would not be much difference in pixel reflectance values between skim ice and open water pixels, while a visual inspection would spot the skim ice forming through a change in surface texture in the imagery. The final ice-on was the opposite, as we can see small areas with no ice that are later than the classification can detect. The first ice-off dates were the most similar between the methods, but still presented challenges, as the subtle nearshore changes at the beginning of breakup can be difficult to distinguish. Final ice-off was a little later using the manual method. Similar to the ice-on, this related to how much better ice could be distinguished visually compared to the classified method. Differences in snow dates are similar to those in ice in that, visually, we can detect small patches, or thin scatterings, of snow cover, leading to, for example, larger discrepancies in the snow-on timing.

Another aspect to consider is the subjectivity of visual analysis used for validating the classification method. To reduce subjectivity errors, we recommend that at least two people assess imagery when using manual extraction techniques. Visual observation of snow and ice phenology by researchers is common (e.g., Ansari et al., 2017; Han et al., 2020), and the goal of this research was to develop an automated method to handle a large volume of data while retaining expert ground-based interpretation of the imagery. Despite the small differences in dates obtained through each technique, overall durations were quite similar. This study demonstrated the utility of ground-based imagery, as finer resolution captures small changes, such as snow-free ground in May, that are not detectable from most satellite-based platforms. Furthermore, this blend of remote sensing and ground-based data could be very beneficial for obtaining finer-resolution data than is obtainable from space, or for validating space-based or modelling work, which is extremely challenging in remote Arctic locations (e.g., Murfitt et al., 2018; Robinson and Brown, 2025).

Some of the years where the classification method had larger differences compared to the manually observed dates can be attributed to camera placement and can be alleviated in future studies. For example, at Small Lake, the camera was too close to the shoreline, which posed difficulties during melt, when the water level changed, overflowing the shoreline. This camera has since been relocated to a higher position on the surrounding hill. Challenges with the cameras tipping or rotating during the season (e.g., Plateau Lake) have since been reduced; the current setup of cameras uses a T-bar, rather than rebar, allowing for a flat surface on which the camera can be more securely mounted.

Future research can explore several possibilities to improve classification. Transition periods remain an area for improvement in classification results (e.g., thin skim ice in the fall, or wet melting ice in spring). Reducing cloud-related misclassification errors is possible through more refined image masking to eliminate the sky from the analysis; with improved camera stability, this will be possible in future work. Our overall methods are not program-specific and can be recreated with other software to further enhance their effectiveness and increase efficiency through additional automation. Although this analysis was conducted in ERDAS Imagine, other image classification software could be used to recreate the workflow, with or without the georectification step included (e.g., open-source QGIS, ArcPro, or even adapted for direct coding software, such as Python). Further automation may also be possible for future work through a temporal consistency check to flag or remove misclassifications that would more than likely be due to errors, for example, open water detected during a typically ice-covered period, though thorough knowledge of the region's climate and the seasonal variability experienced would be required.

To further build on this work, the addition of a snow stake to monitor snow depth changes within the camera view would be extremely beneficial. The snow stake would serve as a ground-truthing tool and enable measuring snow accumulation; however, this was not possible for this study, as the stakes would pose a safety hazard to snowmobilers in the area. For future deployments, optimal camera setups would keep the camera orientation offset from the seasonal sun azimuth, use elevated ridges or higher positions, where possible, and maintain consistent geometry across years to support comparison. Additionally, care should be taken to ensure the camera is securely mounted to the mounting post; we now use bolts through T-bar in most cases, but if cold weather zip ties are being used, consider adding a mounting strap (e.g., those that come with trail cameras intended to be used on trees) as well, to help reduce camera movement in extreme weather.

While logistics can limit the number of cameras around a lake, having more than one camera per lake (or a network of cameras surrounding a lake), or using any topographic advantages possible to position the cameras for lake-wide views, could provide an even more in-depth comparison of spatial variability and subpixel analysis for satellite-based work.

Arctic research presents numerous logistical challenges; however, monitoring changes in lake ice and snow will become an increasingly important priority in a rapidly warming Arctic environment. Ground-based automated cameras alleviate some of these monitoring restraints and provide incredibly valuable insight into spatial conditions in such remote locations. They also add confidence to space-based or modelling-based phenology work. Further, these methods could be adapted to maintain near-real time updates on ice road conditions using shoreline cameras (where cellular or satellite capabilities permit). Such an adaptation of the method could be important to support economic resilience and security in Canada and other countries in the Northern Hemisphere where snow and ice play a crucial role in the environment.

ACKNOWLEDGEMENTS

This project was funded by an NSERC Discovery Grant and the Northern Scientific Training Program, with logistical support through the Polar Continental Shelf Program. We would like to thank Debbie Iqaluk, Noah Bacal, Daniel Serrano-Cadena, and Xiaomeng Zuo for field assistance, and Alex Cabaj for suggestions to strengthen an early draft of this manuscript.

During the preparation of this work, the authors used the software Grammarly to assist with proofreading for grammatical errors and typos in the manuscript. After using this tool, the author(s) reviewed and edited the content as needed and take full responsibility for the content of the publication.

REFERENCES

Anderson, C.M., Fahrig, L., Rausch, J., Martin, J-L., Daufresne, T., and Smith, P.A., 2023. Climate-related range shifts in Arctic-breeding shorebirds. Ecology and Evolution 13(2): e9797.
https://doi.org/10.1002/ece3.9797

Ansari, S., Rennie, C.D., Seidou, O., Malenchak, J., and Zare, S.G. 2017. Automated monitoring of river ice processes using shore-based imagery. Cold Region Science and Technology 142:1–16.
https://doi.org/10.1016/j.coldregions.2017.06.011

Ariano, S.S., and Brown, L.C. 2019. Ice processes on medium-sized north-temperate lakes. Hydrological Processes 33(18):2434–2448.
https://doi.org/10.1002/hyp.13481

Arp, C.D., Jones, B.M., Whitman, M., Larsen, A., and Urban, F.E. 2010. Lake temperature and ice cover regimes in the Alaskan subarctic and Arctic: Integrated monitoring, remote sensing, and modeling. JAWRA Journal of the American Water Resources Association 46(4):777–791.
https://doi.org/10.1111/j.1752-1688.2010.00451.x

Atkinson, D.M., and Treitz, P. 2012. Arctic ecological classifications derived from vegetation community and satellite spectral data. Remote Sensing 4(12):3948–3971.
https://doi.org/10.3390/rs4123948

Benson, B.J., Magnuson, J.J., Jensen, O.P., Card, V.M., Hodgkins, G., Korhonen, J., Livingstone, D.M., Stewart, K.M., Weyhenmeyer, G.A., and Granin, N.G. 2012. Extreme events, trends, and variability in Northern Hemisphere lake-ice phenology (1855–2005). Climate Change 112(2):299–323.
https://doi.org/10.1007/s10584-011-0212-8

Bokhorst, S., Pedersen, S.H., Brucker, L., Anisimov, O., Bjerke, J.W., Brown, R.D., Ehrich, D., et al. 2016. Changing Arctic snow cover: A review of recent developments and assessment of future needs for observations, modelling, and impacts. Ambio 45(5):516–537.
https://doi.org/10.1007/s13280-016-0770-0

Bothmann, L., Menzel, A., Menze, B.H., Schunk, C., and Kauermann, G. 2017. Automated processing of webcam images for phenological classification. PLoS One 12(2): 0171918.
https://doi.org/10.1371/journal.pone.0171918

Brereton, R.G. 2021. Contingency tables, confusion matrices, classifiers and quality of prediction. Journal of Chemometrics35(11): e3331.
https://doi.org/10.1002/cem.3331

Brown, L.C., and Duguay, C.R. 2010. The response and role of ice cover in lake-climate interactions. Progress in Physical Geography 34(5):671–704.
https://doi.org/10.1177/0309133310375653

Brown, R.D., Smith, C., Derksen, C., and Mudryk, L. 2021. Canadian in situ snow cover trends for 1955–2017 including an assessment of the impact of automation. Atmosphere – Ocean 59(2):77–92.
https://doi.org/10.1080/07055900.2021.1911781

Canadian Wildlife Service. 2001. Information sheet on Ramsar Wetlands. Accessed 30 November 2022.
https://rsis.ramsar.org/RISapp/files/RISrep/CA245RIS.pdf

Chasmer, L., Hopkinson, C., Veness, T., Quinton, W., and Baltzer, J. 2014. A decision-tree classification for low-lying complex land cover types within the zone of discontinuous permafrost. Remote Sensing of Environment 143(5):73–84.
https://doi.org/10.1016/j.rse.2013.12.016

Congalton, R.G. 1991. A review of assessing the accuracy of classifications of remotely sensed data. Remote Sensing of Environment 37(1):35–46.
https://doi.org/10.1016/0034-4257(91)90048-B

Dauginis, A.L.A., Brown, L.C. 2020. Sea ice and snow phenology in the Canadian Arctic Archipelago from 1997 to 2018. Arctic Science 7(1):182–207.
https://www.sciencedirect.com/science/article/abs/pii/003442579190048B?via%3Dihub

Dauginis, A., and Brown, L. 2021. Recent changes in pan-Arctic sea ice, lake ice, and snow on/off timing. The Cryosphere 15(10):4781–4805. https://doi.org/10.5194/tc-2021-52

Du, J., Kimball, J.S., Duguay, C., Kim, Y., and Watts, J.D. 2017. Satellite microwave assessment of Northern Hemisphere lake ice phenology from 2002 to 2015. The Cryosphere 11(1):47–63. https://doi.org/10.5194/tc-11-47-2017

Dugan, H.A., Lamoureux, S.F., Lewis, T., and Lafrenière, M.J. 2012. The impact of permafrost disturbances and sediment loading on the limnological characteristics of two High Arctic lakes. Permafrost and Periglacial Processes 23(2):119–126. https://doi.org/10.1002/ppp.1735

ECCC (Environment and Climate Change Canada). 2022. Historical climate data. Accessed 6 December 2021. https://climate.weather.gc.ca/index_e.html

Enderle, D.I., and Weih, R.C., Jr. 2005. Integrating supervised and unsupervised classification methods to develop a more accurate land cover classification. Journal of the Arkansas Academic Sciences 59: 10. https://scholarworks.uark.edu/cgi/viewcontent.cgi?article=1535&context=jaas

French, H., and Slaymaker, O. 2011. Changing cold environments: A Canadian perspective. Hoboken, New Jersey: Wiley-Blackwell.

Geldsetzer, T., van der Sanden, J., and Brisco, B. 2010. Monitoring lake ice during spring melt using RADARSAT-2 SAR. Canadian Journal of Remote Sensing 36(sup 2):S391–S400. https://doi.org/10.5589/m11-001

Hampton, S.E., Galloway, A.W.E., Powers, S.M., Ozersky, T., Woo, K.H., Batt, R.D., Labou, S.G., et al. 2017. Ecology under lake ice. Ecology Letters 20(1):98–111. https://doi.org/10.1111/ele.12699

Han, W., Huang, C., Duan, H., Gu, J., and Hou, J. 2020. Lake phenology of freeze-thaw cycles using random forest: A case study of Qinghai Lake. Remote Sensing 12(24): 4098. https://doi.org/10.3390/rs12244098

Heron, R., and Woo, M.-K. 1994. Decay of a High Arctic lake-ice cover: Observations and modelling. Journal of Glaciology 40(135):283–292. https://doi.org/10.1017/S0022143000007371

Hexagon. 2024. ERDAS documentation, field producers guide. Accessed March 2026. https://hexagongeospatial.fluidtopics.net/r/uOKHREQkd_XR9iPo9Y_Ijw/khBQoaH4ne8R6PVMWZ7Ubw.

Howell, S.E.L., Assini, J., Young, K.L., Abnizova, A., and Derksen, C. 2012. Snowmelt variability in Polar Bear Pass, Nunavut, Canada, from QuikSCAT: 2000–2009. Hydrological Processes 26(23):3477–3488. https://doi.org/10.1002/hyp.8365

Huang, L., Timmermann, A., Lee, S.-S., Rodgers, K.B., Yamaguchi, R., and Chung, E.-S. 2022. Emerging unprecedented lake ice loss in climate change projections. Nature Communications 13: 5798. https://doi.org/10.1038/s41467-022-33495-3

Hung, J.K.Y., and Treitz, P. 2020. Environmental land-cover classification for integrated watershed studies: Cape Bounty, Melville Island, Nunavut. Arctic Science 6(4):404–422. https://doi.org/10.1139/as-2019-0029

Kimes, D.S. 1983. Dynamics of directional reflectance factor distributions for vegetation canopies. Applied Optic 22(9):1364–1372. https://doi.org/10.1364/AO.22.001364

Latifovic, R., and Pouliot, D. 2007. Analysis of climate change impacts on lake ice phenology in Canada using the historical satellite data record. Remote Sensing of Environment 106(4):492–507. https://doi.org/10.1016/j.rse.2006.09.015

Lenormand, F., Duguay, C.R., and Gauthier, R. 2002. Development of a historical ice database for the study of climate change in Canada. Hydrological Processes 16(18):3707–3722. https://doi.org/10.1002/hyp.1235

Lescord, G.L., Kidd, K.A., Kirk, J.L., O'Driscoll, N.J., Wang, X., and Muir, D.C.G. 2015. Factors affecting biotic mercury concentrations and biomagnification through lake food webs in the Canadian high Arctic. Science of the Total Environment 509-510:195–205. https://doi.org/10.1016/j.scitotenv.2014.04.133

Leshkevich, G., and Nghiem, S.V. 2013. Great Lakes ice classification using satellite C-band SAR multi-polarization data. Journal of Great Lakes Research 39(S1):55–64. https://doi.org/10.1016/j.jglr.2013.05.003

Liston, G.E., and Hiemstra, C.A. 2011. The changing cryosphere: Pan-Arctic snow trends (1979–2009). Journal of Climate 24(21):5691–5712. https://doi.org/10.1175/JCLI-D-11-00081.1

MacKay, M.D., Verseghy, D.L., Fortin, V., and Rennie, M.D. 2017. Wintertime simulations of a boreal lake with the Canadian small lake model. Journal of Hydrometeorology 18(8):2143–2160. https://doi.org/10.1175/JHM-D-16-0268.1

McCrystall, M., Stroeve, J., Serreze, M., Forbes, B., and Screen, J. 2021. New climate models reveal faster and larger increases in Arctic precipitation than previously projected. Nature Communications 12: 6765.
https://doi.org/10.1038/s41467-021-27031-y

Mohd Hasmadi, I., Pakhriazad, H.Z., and Shahrin, M.F. 2009. Evaluating supervised and unsupervised techniques for land cover mapping using remote sensing data. Malaysian Journal of Society and Space 5(1).
https://www.proquest.com/openview/3ce55d3fe96fef40bc5d5167ff0f18f2/1?pq-origsite=gscholar&cbl=4916363

Mudryk, L.R., Derksen, C., Howell, S., Laliberté, F., Thackeray, C., Sospedra-Alfonso, R., Vionnet, V., Kushner, P.J., and Brown, R. 2018. Canadian snow and sea ice: Historical trends and projections. The Cryosphere 12(4):1157–1176.
https://doi.org/10.5194/tc-12-1157-2018

Mudryk, L., Santolaria-Otín, M., Krinner, G., Ménégoz, M., Derksen, C., Brutel-Vuilmet, C., Brady, M., and Essery, R. 2020. Historical Northern Hemisphere snow cover trends and projected changes in the CMIP6 multi-model ensemble. The Cryosphere 14(7):2495–2514.
https://doi.org/10.5194/tc-14-2495-2020

Mudryk, L., Elias Chereque, A., Derksen, C., Luojus, K., and Decharme, B. 2022. Arctic report card 2022: Terrestrial snow cover. NOAA technical report OAR ARC 22-03.
https://doi.org/10.25923/yxs5-6c72

Murfitt, J., and Duguay, C.R. 2021. 50 years of lake ice research from active microwave remote sensing: Progress and prospects. Remote Sensing of Environment 264: 112616.
https://doi.org/10.1016/j.rse.2021.112616

Murfitt, J., Brown, L.C., and Howel, S.E.L. 2018. Evaluating RADARSAT-2 for the monitoring of lake ice phenology events in mid-latitudes. Remote Sensing 10(10): 1641.
https://doi.org/10.3390/rs10101641

Nicodemus, F., Richmond, J., Hsia, J., Ginsberg, I., and Limperis, T. 1977. Geometrical considerations and nomenclature for reflectance. U.S. Department of Commerce, National Board of Standards Monograph 160.
https://nvlpubs.nist.gov/nistpubs/Legacy/MONO/nbsmonograph160.pdf

Parker, J.A., Kenyon, R.V., and Troxel, D.E. 1983. Comparison of interpolating methods for image resampling. IEEE Transactions on Medical Imaging 2(1):31–39.
https://doi.org/10.1109/TMI.1983.4307610

Prowse, T., Alfredsen, K., Beltaos, S., Bonsal, B., Duguay, C., Korhola, A., McNamara, J., Vincent, W.F., Vuglinsky, V., and Weyhenmeyer, G.A. 2011. Arctic freshwater ice and its climatic role. Ambio 40:46–52.
https://doi.org/10.1007/s13280-011-0214-9

Rantanen, M., Karpechko, A.Y., Lipponen, A., Nordling, K., Hyvärinen, O., Ruosteenoja, K., Vihma, T., and Laaksonen, A. 2022. The Arctic has warmed nearly four times faster than the globe since 1979. Communications Earth & Environment 3: 168.
https://doi.org/10.1038/s43247-022-00498-3

Robinson, A.L., and Brown, L.C. 2025. Simulated current and projected radiation balance of a High Arctic lake during the open water season. Arctic Science 11:1–22.
https://doi.org/10.1139/as-2024-0081

Robinson, A.L., Ariano, S.S., and Brown, L.C. 2021. The influence of snow and ice albedo towards improved lake ice simulations. Hydrology 8(1): 11.
https://doi.org/10.3390/hydrology8010011

Serreze, M.C., and Barry, R.G. 2014. The Arctic climate system. Cambridge: Cambridge University Press.

Smith, P.A., Gilchrist, H.G., Forbes, M.R., Martin, J., and Allard, K., 2010. Inter-annual variation in the breeding chronology of Arctic shorebirds: Effects of weather, snow melt and predators. Journal of Avian Biology 41:292–304.
https://doi.org/10.1111/j.1600-048X.2009.04815.x

Surdu, C.M., Duguay, C.R., and Prieto, D.F. 2016. Evidence of recent changes in the ice regime of lakes in the Canadian High Arctic from spaceborne satellite observations. The Cryosphere 10(3):941–960.
https://doi.org/10.5194/tc-10-941-2016

Tom, M., Prabha, R., Wu, T., Baltsavias, E., Leal-Taixé, L., and Schindler, K. 2020. Ice monitoring in Swiss lakes from optical satellites and webcams using machine learning. Remote Sensing 12(21): 3555.
https://doi.org/10.3390/rs12213555

Wang, X., Feng, L., Qi, W., Cai, X., Zheng, Y., Gibson, L., Tang, J., et al. 2022. Continuous loss of global lake ice across two centuries revealed by satellite observations and numerical modeling. Geophysical Research Letters 49(12): e2022GL099022.
https://doi.org/10.1029/2022GL099022

Wu, Y., Duguay, C.R., and Xu, L. 2021. Assessment of machine learning classifiers for global lake ice cover mapping from MODIS TOA reflectance data. Remote Sensing of Environment 253: 112206.
https://doi.org/10.1016/j.rse.2020.112206

Xiao, M., Rothermel, M., Tom, M., Galliani, S., Baltsavias, E., and Schindler, K. 2018. Lake ice monitoring with webcams. ISPRS Annals of the Photogrammetry, Remote Sensing and Spatial Information Sciences IV-2:311–317.
https://doi.org/10.5194/isprs-annals-IV-2-311-2018

Young, K.L., and Labine, C. 2010. Summer hydroclimatology of an extensive low-gradient wetland: Polar Bear Pass, Bathurst Island, Nunavut, Canada. Hydrology Research 41(6):492–502.
https://doi.org/10.2166/nh.2010.219

Young, K.L., and Brown, L.C. 2023. Temperature and precipitation trends of the shoulder seasons at Polar Bear Pass (Nanuit Itillinga) – A Ramsar wetland of importance, Nunavut. Wetlands 43(68).
https://doi.org/10.1007/s13157-023-01712-4

Young, K.L., Brown, L., and Labine, C. 2018. Snow cover variability at Polar Bear Pass, Nunavut. Arctic Science 4(4):669–690.
https://doi.org/10.1139/as-2017-0016

Young, S.S. 2023. Global and regional snow cover decline: 2000–2022. Climate 11(8): 162.
https://doi.org/10.3390/cli11080162

Zhang, S., Pavelsky, T.M., Arp, C.D., and Yang, X. 2021. Remote sensing of lake ice phenology in Alaska. Environmental Research Letters 16(6): 064007.
https://doi.org/10.1088/1748-9326/abf965